The International Journal of Advanced Manufacturing Technology
https://doi.org/10.1007/s00170-024-13087-9

ORIGINAL ARTICLE

A comparative machinability analysis of polyimine vitrimer, epoxy and polycarbonate polymers through orthogonal machining experiments

Dániel István Poór[1,2] · Marina Tobey[3] · Philip Taynton[3] · Ákos Pomázi[2,4] · Andrea Toldy[2,4] · Norbert Geier[1]

Received: 11 September 2023 / Accepted: 21 January 2024

Abstract
End-of-life management of fibre-reinforced thermoset composites is challenging due to the difficult-to-recycle reinforcements and the irreversibly polymerised thermoset matrix; therefore, researchers proposed the vitrimers as a sustainable alternative to thermosetting polymers. Although the early results of the material scientists are promising, the machinability of vitrimers has yet to be explored. Therefore, this paper aims to present a comparative machinability study of polyimine vitrimer, pentaerythritol-based epoxy (PER) and polycarbonate polymers through orthogonal machining experiments. Reflecting on the temperature-dependent properties of vitrimers, the starting temperature of the cutting tool was varied between room temperature and an elevated temperature above 155 °C. The cutting tool was heated by a 2000-W hot air gun until the surface temperature of the cutting tool, monitored by a VariocamHD thermographic IR camera (with Jenoptik IR 1.0/60 LW lens) and checked by a Fluke 51 II thermometer with a type K thermocouple, was permanently above 155 °C for 5 min. The cutting force was measured by a Kistler 9257B dynamometer, and the machined surface was characterised by a Mitutoyo Surftest SJ-400 surface roughness tester and Keyence VHX-5000 (with VH-Z20UT VH lens) microscope. The analysis of variances (ANOVA) results show that the sustainable vitrimer polymer is an appropriate substitute for thermosetting epoxy polymers, especially at low cutting temperatures.

Keywords Vitrimer · Machinability · Orthogonal machining · Cutting force · Surface quality

1 Introduction

Applications of fibre-reinforced polymer (FRP) composites are rapidly growing mainly due to their excellent specific mechanical properties and easy-to-shape behaviour [1–3]. FRP composites are decisive components of high-strength lightweight structures like aeroplanes, ships, space shuttles and wind turbines [4–6]. These high-end applications usually require using thermosetting polymers as a matrix material to meet the mechanical requirements. However, the end-of-life management of these thermosetting polymeric fibre-reinforced composites is challenging due to the difficult-to-recycle reinforcements and thermoset matrix, usually produced by an irreversible polymerisation process [7–9]. Therefore, most of the current technical FRP applications are considered less sustainable compared with thermoplastic FRP composites, whose recycling technologies are well-developed. Nowadays, legislation and social demand increasingly encourage sustainability, posing the need to replace thermosetting polymers with more sustainable polymers without compromising their beneficial mechanical properties [10–13].

Thermosetting polymers have limited self-healing, reshaping, and recycling capabilities due to their insoluble and infusible nature [8]. To overcome these limitations, covalent adaptable networks (CANs) have been developed.

✉ Norbert Geier
geier.norbert@gpk.bme.hu

1 Department of Manufacturing Science and Engineering, Faculty of Mechanical Engineering, Budapest University of Technology and Economics, Műegyetem Rkp. 3, Budapest 1111, Hungary

2 MTA-BME Lendület Sustainable Polymers Research Group, Műegyetem Rkp. 3, 1111 Budapest, Hungary

3 Mallinda Inc, Denver, CO 80229, USA

4 Department of Polymer Engineering, Faculty of Mechanical Engineering, Budapest University of Technology and Economics, Műegyetem Rkp. 3, Budapest 1111, Hungary

Published online: 07 February 2024

CANs incorporate reversible covalent bonds and can be categorised based on their bond exchange mechanism—dissociative or associative. In dissociative CANs, such as polymers based on Diels–Alder reactions, bonds break and reform, leading to reduced viscosity and dimensional stability. In contrast, associative CANs form new bonds before breaking the existing ones, maintaining crosslink density and structural integrity. Vitrimers, introduced by Montarnal et al. [14] in 2011, belong to the associative type of CANs. They behave like crosslinked systems below the glass transition temperature, but they can be reshaped and recycled like thermoplastics above their vitrimeric transition temperature (T_v) [14]. This thermally triggered reversible crosslinking occurs through the dynamic rearrangement of covalent bonds in an associative manner [15]. The most convenient vitrimer bond exchange mechanisms include transesterification, imine exchange and disulfide exchange. These mechanisms allow for network exchanges under diverse environmental conditions, resulting in vitrimers with enhanced mechanical and thermal properties. Taynton et al. [16] prepared a catalyst-free malleable network polymer based on imine chemistry (also known as Schiff base chemistry) from commercially available monomers. Their vitrimer can also be obtained in powder form, and solid vitrimer parts can be processed with heat and pressure in a mould. They examined the recyclability, reshaping and malleability properties of the material, and they observed that the vitrimer had Arrhenius-like malleability as a response to heat; also, the polymer can be recycled and reshaped by only applying water at ambient temperature conditions. They discovered the vitrimer's mechanical properties did not deteriorate significantly after four recycling cycles. Taynton et al. [17], in their further research, prepared CFRP composite sheets from their polyimine-based vitrimer and woven carbon fibre reinforcement. They studied the processibility, reshaping ability, reparability and recyclability of the composites. They successfully produced the composite sheets and could weld multiple composite layers by heat and pressure; the composite sheet was reshaped into a 3D dome form by a moulding process. The matrix and reinforcement materials were fully recovered by a simple recycling procedure, and they were also capable of repairing delamination damage in their CFRP composite workpieces by heat-pressing them. Polyimine-based vitrimers patented in 2019 [18] show potential as replacements for epoxy resins in structural composites due to their high glass transition temperature.

The measurement of glass transition temperature (T_g) is already well-developed in academia and industrial practice. T_g is usually determined by differential scanning calorimetry (DSC) from the second heating of a three-step temperature program consisting of heat/cool/heat cycles according to EN ISO 11357–2:2020 [19]. The T_g is defined as the inflection point of the transition curve. The polymers' T_g can also be determined by dynamic mechanical analysis (DMA); the sensitivity of the measurement is approx. 1000 times higher than in the case of DSC [20]. The value of T_g by DMA can be determined by various methods as follows: (i) the peak value of loss tangent, (ii) the peak value of loss modulus, (iii) the first derivative of the drop of storage modulus and (iv) the onset values of the drop of storage modulus [20]. However, there is no commonly applied standard measurement technique for measuring the vitrimeric transition temperature (T_v); presently, dilatometry test, stress relaxation test by rheology and DMA are used [21]. The applied external force in these measurements shifts the real T_v value, while the crosslinks breakage rate and the effective activation energy will be influenced by the extra tension. Yang et al. [21] added aggregation-induced emission (AIE) luminogens into vitrimers in their research, and they examined the fluorescence change of the AIE-luminogens below and above T_v. They found out that their experimental method has good repeatability and can be carried out fast and simply; also, by avoiding the effect of external forces, measurement data sampled at different conditions may be comparable. Nevertheless, the experimental data of previous researches so far show that the vitrimers's T_v value is usually above the T_g with a few tens of °C [22, 23].

There are several polymer manufacturing technologies available to produce polymer and FRP composite products (e.g., injection moulding, silicone casting, 3D printing, high-pressure resin transfer moulding, hand lamination, vacuum infusion process and prepregging.); however, in many cases (especially in the case of FRP composites manufacturing) further material-removing technologies (e.g., milling, drilling, laser beam cutting, abrasive water jet cutting) must be applied due to the demanded dimensional precision and surface quality. Machining technologies are superior compared to other technologies in industrial practices from the point of view of precision and material removal rate [24–26]. The properties and behaviour of the composites' matrix material during machining highly influence the quality of machined geometrical features. Therefore, the investigation of matrix materials' machinability may help the understanding and modelling of the mechanical processes and outcome of the more complex FRP composite machining [27, 28]. Although the early results on the material properties of vitrimers are very promising, their machinability still needs to be discovered. Considering that the material properties of vitrimers are significantly different below and above the vitrimeric transition temperature (T_v), the glass transition temperature (T_g) has a key role in the mechanical properties; the machinability is also expected to be different at different temperatures. The machinability of vitrimers below the T_v is expected to be similar to that of thermosetting polymers. Nevertheless, if the cutting temperature exceeds the T_v, the polymer becomes softer and behaves like a thermoplastic.

Although the machinability of vitrimers was not investigated yet, researchers gained experience in machining thermosetting (e.g., epoxy resin, polyester resin, vinylester resin, polyimide, bakelite) and thermoplastic (e.g., high-density polyethylene (HDPE), polypropylene (PP), polyetheretherketone (PEEK), polycarbonate (PC) and polyamide 66 (PA66)) polymers [24, 29–37]. For example, Wang et al. [30] conducted orthogonal cutting experiments on different density epoxy samples and examined the cutting mechanisms. Their experimental results agreed with previous researches that the dominant mechanism during chip formation is fracture. The crosslink density affects the chip formation via the effect on the material's post-yield deformability. They also found that the increase in the depth of cut (uncut chip thickness) makes a transition from brittle chipping to ductile continuous chip formation. Fu et al. [29] made micro- and macro-machining FE simulations of epoxy with the Mulliken Boyce model, and they validated their work with empirical experiments. They classified the cutting deformation mechanism as shear plastic slip, and their simulation resulted in three different types of chip shapes: (i) continuous, (ii) serrated, and (iii) broken chips, which chip types were also observed in the empirical experiments. However, the experimental values of cutting forces were higher than the simulated ones. Hanson et al. [36] investigated via experiments and simulated numerically the burr formation of polycarbonates during micro-milling. They found out that the uncoated carbide tool produced less burr formation compared to the TiN- and TiAlN-coated tools except in the case of a very high depth-of-cut of the TiN-coated tool (0.5 mm); however, the coated tools produced better surface quality. It was also shown that in the case of a lower depth of cut, a higher feed rate should be applied and vice versa to minimise burr. Wang et al. [35] measured the fracture toughness of HDPE, PP and PEEK materials via orthogonal cutting tests. The experiments proved that in the range of 100–250 µm depth of cut, there is a linear connection between the measured cutting force values and fracture toughness values; therefore, orthogonal cutting tests are capable of geometry-free fracture toughness measurement. Although, in the case of under 100 µm depth of cut, an inverse size effect can be observed: the fracture energy decreases with the decrease of the depth of cut.

Reflecting on the lack of published experience in the machinability of sustainable vitrimer polymers, the main aim of the present study is to gain preliminary information on the cutting force and machined surface characteristics of the applied polyimine vitrimer through orthogonal machining experiments and compare the results with a selected thermoplastic and thermosetting polymer. As temperature has a key role in the mechanical properties and material structure of polymer materials, especially in the case of the new vitrimer polymers, the effect of elevated temperature on the machinability of the examined materials is also investigated. The results of the machinability analysis and the experience on the vitrimer's behaviour during machining may be implemented in modelling vitrimer matrix FRP composites and could help the understanding of those composites' machinability and support the spread of sustainable applications.

2 Materials and methods

2.1 Polymer materials

The experimental work involved three different types of polymer materials. The initial objective of the research was to explore the machinability properties of vitrimer polymers, in addition to comparing them to the properties of an epoxy resin (thermoset material) with similar T_g and the properties of a polycarbonate (PC) material. The epoxy resin was chosen because vitrimer polymers are a potential substitute for epoxies. The PC was selected for its excellent mechanical properties (high strength and stiffness, good impact resistance and dimensional stability) and the amorphous polymer structure, which is more suitable for comparison to elastomers and vitrimers than a crystalline or semi-crystalline polymer. Crystalline and semi-crystalline polymers are usually applied between their T_g and T_m (melting temperature); also, the recrystallisation process can occur during temperature increase or mechanical impact, which can significantly change the material's mechanical properties during machining.

The vitrimer and epoxy samples were cast in silicone moulds. For the polyimine vitrimer samples, the two-component VITRIMAX T130 system was used (produced by Mallinda Inc., (Denver, CO, USA)). Firstly, the polyimine hardener was heated to 80 °C for 1 h to lower its viscosity before the mixing procedure. After that, the polyimine hardener was mixed with the epoxy resin system; the mixing ratio of the polyimine hardener and epoxy resin was 2:1. Then, the mixture was poured into the silicone mould; the liquid vitrimer system was treated carefully with a hot air gun to reduce the bubble content. A glass sheet was placed on top of the silicone mould to ensure the constant thickness of the samples. The curing happened at room temperature for 24 h; also, post-curing was applied at 80 °C for 2 h in a Heraeus UT20 drying oven (Hanau, Germany). For the epoxy resin samples, the two-component MR3016/MH3122 PER epoxy system was used (epoxy monomer, pentaerythritol tetraglycidyl ether; hardener, 3,3′-dimethyl-4,4′-diaminodicyclohexylmethane; produced by Ipox Chemicals (Budapest, Hungary)). The two components were mixed at room temperature with a mixing ratio of 100:40. The epoxy resin was also poured into the silicone mould, which had the same hot air gun treatment for bubble content reduction, and

the glass sheet was also applied for constant sample thickness. The curing and post-curing processes were the same as in the case of polyimine vitrimer. The PC samples were manufactured by injection moulding with an Arburg Allrounder Advance 270S 400–170 injection moulder machine (Lossburg, Germany) from Makrolon 2405 material (produced by Covestro AG (Leverkusen, Germany)). The most important injection moulding parameters are the following: 30 mm screw diameter, 45 cm^3/s injection speed, 400 kN clamping force, 1200 bar injection pressure limit, 8 s holding time, 20 s cooling time, 45 cm^3 of dose volume, 310 °C melt temperature and 80 °C mould temperature.

The manufactured polymer sheets were then cut into 16 × 15 × 4 mm pieces using a Mutronic Diadisc 5200 cut-off saw (Rieden am Forggensee, Germany). The size of the workpieces was iterated empirically based on (i) the geometry of the fixture, (ii) the length of the cutting edge (the thickness of the workpiece must be smaller than the main cutting edge), (iii) the strength of the materials (the material must not break during machining with the applied cutting parameters), (iv) sampling limit of measuring devices, (v) cooling time of the cutting insert and (vi) the cost of materials (due to cost efficiency, material usage should have been minimised). Finally, these polymers were one by one fixed into a special orthogonal fixture (see Fig. 1) and flat milled by a TOS Kuřim FNK 25A (Kuřim, Czech Republic) milling machine (using a face milling cutter having a diameter of 40 mm and cutting inserts having rake angle of 0°, using a nominal depth of cut of 3 mm, cutting speed of 113 m/min and feed rate of 80 mm/min.) to provide a flat starting surface resulting in a uniform size of uncut chip thickness.

The glass transition temperature (T_g) of the examined polymers, produced at our laboratory and with our technology, was measured by dynamic mechanical analysis (DMA) to determine the elevated temperature value of the machining experiments. The DMA was performed by TA Instruments' DMA Q800 instrument (New Castle, Delaware, USA), and the T_g values were determined as the peak values of tanδ signals in the TA Universal Analysis 2000 software. The DMA was carried out with a 3-point bending setup, and the oscillation frequency was 1.00 Hz; the static force was 0.10 N; the minimum oscillation force was 0.00 N; a 1.25-force

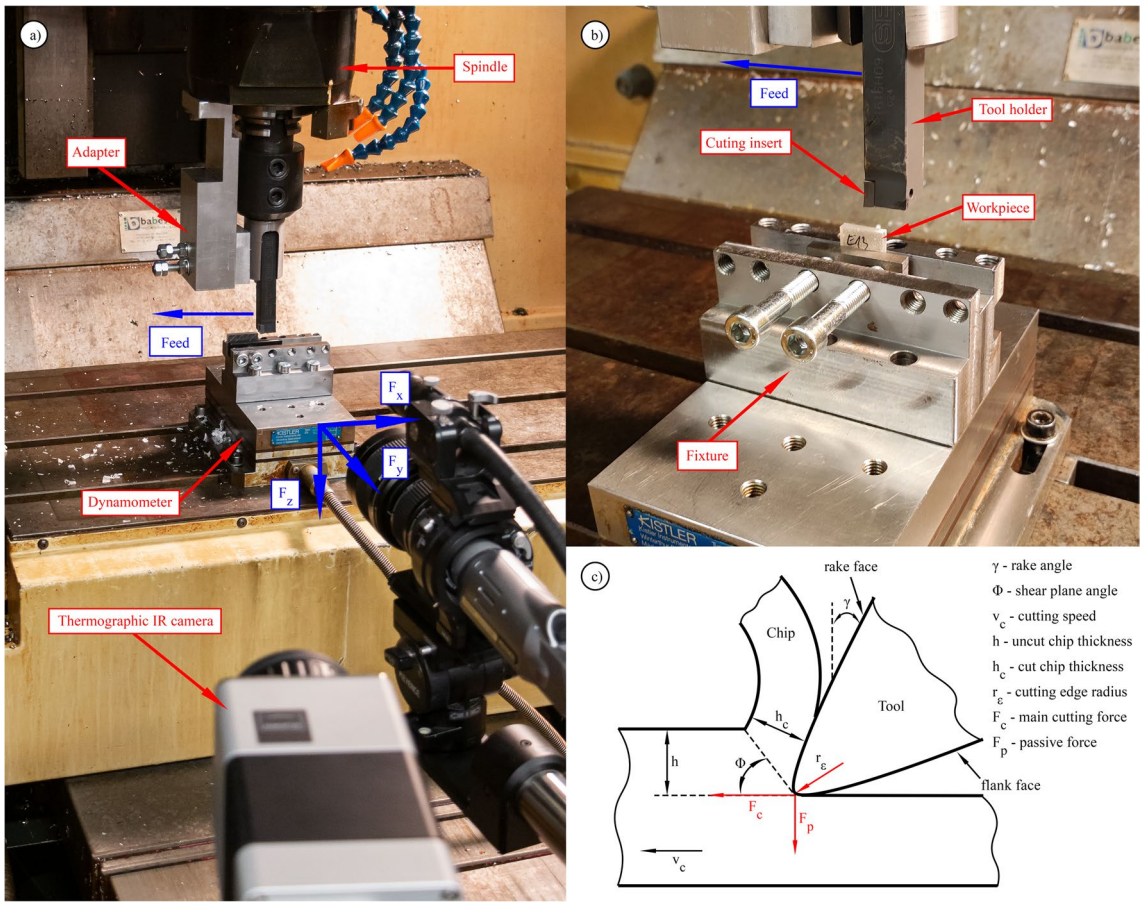

Fig. 1 **a** The orthogonal experimental setup, **b** the setup of the orthogonal cutting process and **c** a schematic figure of orthogonal chip-removing with the most important parameters

track was applied; the oscillation strain was 0.01 mm; the examined temperature range was 28–180 °C, and the heating rate was 3 °C/min. The nominal dimension of the DMA samples was 60 × 10 × 4 mm, and the support span was 50 mm. The T_g and the storage modulus (E') values at 28 °C and at 155 °C of the polymers produced with the technologies mentioned above were produced at our laboratory with our technology and can be seen in Table 1.

2.2 Experimental setup

The orthogonal machining experiments were conducted on a Kondia B640 vertical CNC milling machine (Elgoibar, Spain) in dry conditions. The polymer workpieces were fixed into a unique fixture on a KISTLER 9257B dynamometer (Winterthur, Switzerland), as can be seen in Fig. 1b. The linear movement of the *x*-axis (table movement along the longer planar axis) of the cutting tool machine provided the cutting speed (v_c) for the orthogonal machining experiments. A SECO CCGT09T304F-AL, KX cutting insert (Budapest, Hungary) performed the chip removal so that the main cutting edge was set parallel to the top of the polymer workpieces using a 5°-wedge. The cutting insert was fixed into a SECO SCLCR1616H09 tool holder (Budapest, Hungary) and an adapter. The main cutting edge of the cutting insert was positioned perpendicular to the cutting speed motion (along the *y*-axis of the cutting tool machine) using a Mitutoyo 513–445 (Kawasaki, Japan) measuring clock (precision 2 µm). The orthogonal experimental setup can be seen in Fig. 1.

The cutting force components along the cutting motion and passive directions were measured by a KISTLER 9257B three-component dynamometer using a measurement limit of 500 N and a sampling frequency of 10 kHz. The measured signal was amplified by a KISTLER 5070A11100 multichannel laboratory charge amplifier (Winterthur, Switzerland) and collected by a NI USB-4431 dynamic signal acquisition module (Austin, TX, USA). The temperature of the cutting insert was monitored by a Variocam HD thermographic IR camera (by Jenoptik (Jena, Germany), with a Jenoptik IR 1.0/60 LW lens) using a frame rate of 30 fps and emission coefficient of 0.95. The temperature condition of the cutting insert was manipulated by a PARKSIDE PHLG 2000 E4 hot air gun (Einhell Germany AG, Landau/Isar, Germany) with a performance of 2000 W, nominal air temperature of 550 °C and volume flow of 500 l/min. The temperature of the insert was also checked by a Fluke 51 II thermometer (Everett, WA, USA) with a type-K thermocouple (from Rhodium Kft., Budapest, Hungary).

Considering that the chip removal is expected to be different in significantly different cutting temperatures, and the length of cutting (approx. 30 mm) cannot ensure a significant cutting temperature increase during the experiments, the starting temperature of the cutting insert (T) was selected as a factor besides the material type (M). Due to the relatively low number of factors, the orthogonal machining experiments were designed according to the full factorial design by repeating each experimental run five times. The T was varied between two categorical levels, i.e., room temperature and elevated temperature, above 155 °C. This elevated temperature was set to be above the examined polymer's T_g and the vitrimer's T_v temperatures; T_v is difficult to measure accurately, but from the T_g of the vitrimer and based on previous research, it is a few tens of °C higher than the T_g. The factors and their levels are shown in Table 2. A total number of 30 experiments were run in a randomised order to minimise the systematic effect of fixed parameters and conditions. The nominal uncut chip thickness (h) was 0.1 mm (determined by the common values in the case of CFRP drilling and milling processes [38, 39]), and the cutting speed (v_c) was fixed—considering the maximal speed of the *x*-axis of the machine tool—to 20 m/min.

2.3 Characterising parameters

The measured cutting force components were parallel to the *x*-, *y*- and *z*-axes of the CNC cutting machine tool because the axes of the coordinate system of the dynamometer matched

Table 1 Glass transition temperature and storage modulus results of DMA tests

Polymer material	Material properties		
	T_g (°C)	$E'_{28\ °C}$ (MPa)	$E'_{155\ °C}$ (MPa)
PER epoxy	55.00	2157	33.54
Polyimine vitrimer	75.16	1859	0.67
PC	149.66	1327	25.50

Table 2 Factors and their levels

Factors		Levels		
		1	2	3
Starting temperature of the cutting insert	T (°C)	Room temperature (~21 °C)	Above 155 °C	
Material type	M (−)	Polyimine vitrimer (*V*)	PER epoxy resin (*E*)	Polycarbonate (PC)

that of the CNC machine tool (see Fig. 1). Considering that the machining experimental setup ensured the classical implementation of two-dimensional orthogonal machining, only the main cutting force (F_c) and the passive force (F_p) components were evaluated, as expressed by Eqs. (1) and (2), respectively.

$$F_c = \frac{1}{n}\sum_{i=0}^{n}\left|F_{xmin}\right|_i \quad (1)$$

$$F_p = \frac{1}{n}\sum_{i=0}^{n}\left|F_{zmax}\right|_i \quad (2)$$

where $n = 5$ denotes the number of experiment repetitions, i is the increment variable of each experimental run, F_{xmin} denotes the minimum of the x-directional cutting force component, and F_{zmax} denotes the maximum of the z-directional cutting force component. Due to the relatively small applied uncut chip thickness resulting in relatively small cutting forces, the raw cutting force data was not filtered to keep as much information on the chip-removal process as possible. The measured force values can be seen in Table 3 and Figs. 2 and 3.

The machined surface characteristics were analysed through optical microscopy (i.e., qualitative evaluation) with a Keyence VHX-5000 (with VH-Z20UT VH lens, 20–200 × zoom) optical microscope (Osaka, Japan) and contact profilometry with a Mitutoyo Surftest SJ-400 contact profilometer (Kawasaki, Japan) based on EN ISO 4288 standard. The cut-off frequency was set to 8 mm, the measuring speed was set to 0.5 mm/s, and a Gauss filtering was applied. The average surface roughness (Ra), the maximum height of the profile (Rt) and their combination (Rt/Ra) were selected to characterise the machined surfaces qualitatively. The surface profile of each machined sample was measured three times in three different representative locations, their mean value is the associated value to each sample, and the

Table 3 Force and surface roughness results of orthogonal machining experiments

Factors		Optimisation parameters				
Material (M)	Temperature (T)	$F_{x,min}$ (N)	$F_{z,max}$ (N)	Ra (μm)	Rt (μm)	Rt/Ra (1)
E	Room temp	162.86	37.00	47.17	243.90	5.17
E	Room temp	94.92	41.86	30.41	188.73	6.21
E	Room temp	141.35	47.33	41.03	233.97	5.70
E	Room temp	104.49	114.10	40.43	209.83	5.19
E	Room temp	27.51	51.47	48.62	320.73	6.60
E	Above 155 °C	26.17	121.94	71.42	330.50	4.62
E	Above 155 °C	117.94	40.77	86.57	348.53	4.03
E	Above 155 °C	30.20	237.29	56.18	288.03	5.13
E	Above 155 °C	25.22	105.60	48.78	242.80	4.98
E	Above 155 °C	30.28	149.92	72.68	372.10	5.12
V	Room temp	84.55	47.59	0.80	23.20	28.88
V	Room temp	98.36	41.08	3.49	60.07	17.21
V	Room temp	101.67	54.54	3.84	52.87	13.78
V	Room temp	99.69	48.53	1.25	31.23	24.92
V	Room temp	55.95	49.74	7.15	65.57	9.17
V	Above 155 °C	125.78	48.62	50.84	227.01	4.47
V	Above 155 °C	112.46	48.46	42.36	178.83	4.22
V	Above 155 °C	29.07	70.25	35.28	209.07	5.93
V	Above 155 °C	28.65	107.25	31.87	169.63	5.32
V	Above 155 °C	28.54	114.28	42.73	184.57	4.32
PC	Room temp	104.49	48.61	1.12	11.43	10.21
PC	Room temp	102.20	44.84	0.91	8.80	9.67
PC	Room temp	54.29	43.06	3.63	41.40	11.40
PC	Room temp	110.47	51.68	1.24	10.40	8.41
PC	Room temp	63.08	46.11	3.56	35.83	10.07
PC	Above 155 °C	159.66	48.57	1.42	15.73	11.05
PC	Above 155 °C	30.11	68.05	1.60	13.20	8.27
PC	Above 155 °C	29.22	79.64	1.09	10.50	9.63
PC	Above 155 °C	33.37	67.53	1.15	9.90	8.63
PC	Above 155 °C	29.92	85.28	1.53	12.47	8.15

mean value of the different samples' surface roughness values are shown in Fig. 4 and Table 3.

3 Results and discussion

Table 3 summarises the experimental setup, measured and calculated optimisation parameters.

3.1 Analysis of cutting force

Figure 2 shows the calculated cutting force components with a total of one sigma (equals the standard deviation) error bar in orthogonal machining of vitrimer, epoxy and PC polymers at room temperature and elevated temperature above 155 °C. The orthogonal machining of epoxy resulted in the largest main cutting force (F_c) at room temperature, followed by the vitrimer and PC, respectively. Above 155 °C, the vitrimer resulted in the largest F_c, followed by the PC and epoxy. The larger the main cutting force, the larger the resistance of the polymer against machining. Considering that the main cutting force is proportional to the frictional force at the rake and clearance surfaces of the cutting tool, the speed of tool wear is expected to be accelerated at larger forces [40, 41]. Therefore, the larger the main cutting force, the worse the machinability is, from the point of view of cutting energetics

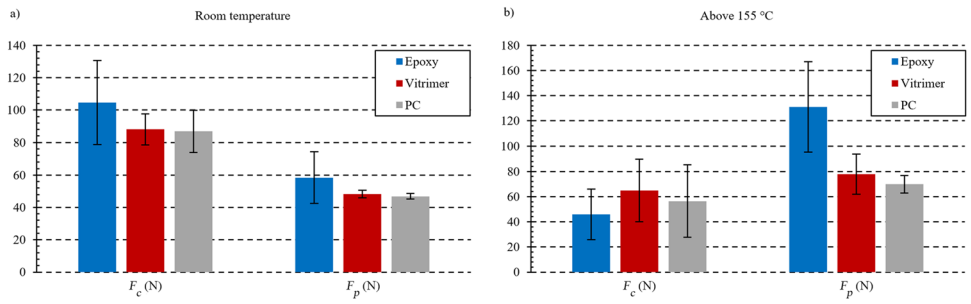

Fig. 2 Cutting force components in orthogonal machining of vitrimer, epoxy and PC polymers at **a** room temperature and **b** above 155 °C

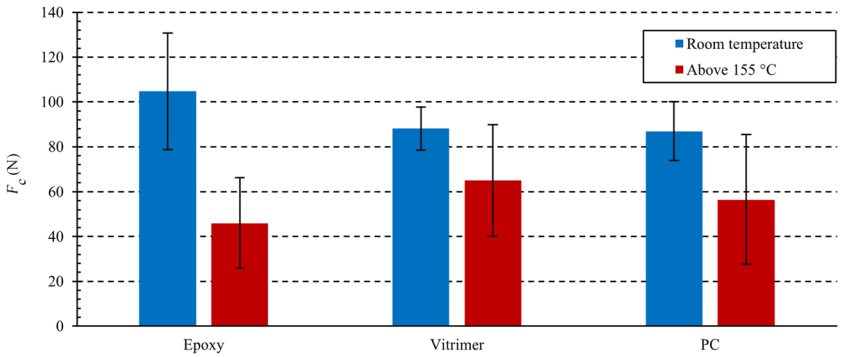

Fig. 3 Main cutting force (F_c) in orthogonal machining of vitrimer, epoxy and PC polymers at room temperature and above the nominal target temperature of 155 °C

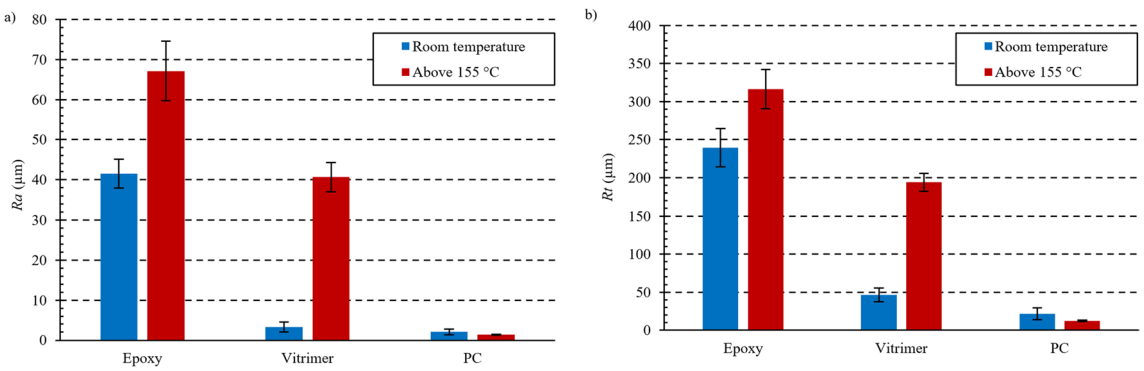

Fig. 4 **a** average surface roughness (Ra) and **b** maximum height of the profile (Rt) of orthogonally machined surfaces of vitrimer, epoxy and PC polymers at room temperature and above 155 °C

and tool wear. Consequently, the vitrimer performed better at room temperature than the epoxy, and the epoxy was more beneficial when the tool was heated above 155 °C. These results suggest that the vitrimer is an appropriate substitute material for epoxy if the cutting temperature is significantly below the glass transition temperature and vitrimeric transition temperature.

The orthogonal machining of epoxy resulted in the largest passive force (F_p) at both analysed temperature conditions. The differences of means of F_p of vitrimer and PC do not differ significantly, but all of them are strictly below the epoxy. The larger the passive force, the dominancy of the peel-up effect caused by the rake surface of the tool is more significant than the ploughing of the cutting edge radius (CER) and clearance surface [42, 43]. Consequently, the results in Fig. 2 indicate that the dominancy of ploughing in the orthogonal machining of vitrimers is more significant than that of the epoxies. The ploughing-induced more considerable compression stress may result in a more hardened and resistant machined surface of vitrimers; however, this needs further investigation.

The analysis of the main cutting force is the most essential among other cutting force components; therefore, it is further detailed and summarised in Fig. 3. The diagram clearly shows that the F_c is larger in every polymer applied at room temperature than above 155 °C. Generally, the mechanical properties of polymers decrease with the temperature increase within the operating temperature range, and a considerable deterioration happens around the polymers' glass transition temperatures (T_g) as the storage modulus (E') values of the DMA tests confirm. Therefore, the main cutting force component is expected to be decreased due to the decrease of the material's resistance against the cutting tool. From the perspective of the positive effects of the decreased F_c (e.g., smaller tool wear and less permanent mechanical damage of the material), the cutting process may be performed at higher temperatures. Still, the material's permanent deterioration must be avoided.

In Figs. 2 and 3, the deviations of the F_c and F_p values highly increase with the increase of the cutting temperature, except in the case of the epoxy material's F_c values. This suggests that the cutting force components become more unpredictable when the temperature during the machining process is indirectly controlled; consequently, tool wear, machine tool maintenance and the machined part's permanent mechanical damage will be difficult to plan and predict.

The main effect and interaction plots can be seen in Figs. 5 and 6, respectively. The means Fig. 5 clearly indicates and is consistent with the previously presented results that the means of the F_c of vitrimer, epoxy and PC do not differ significantly, and the larger the cutting temperature, the smaller the main cutting force is. The

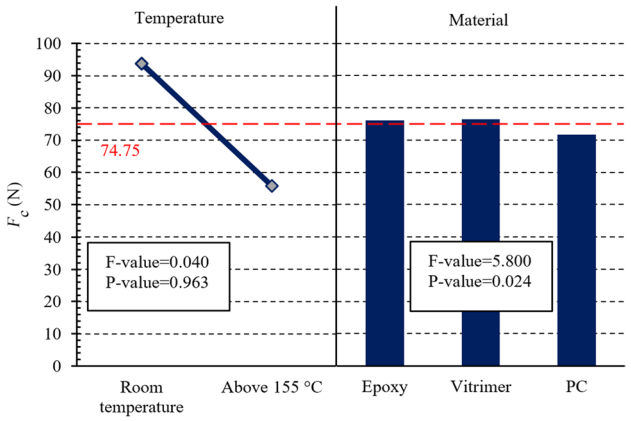

Fig. 5 Main effects plot for main cutting force (F_c) in orthogonal machining of vitrimer, epoxy and PC polymers at room temperature and above the nominal target temperature of 155 °C

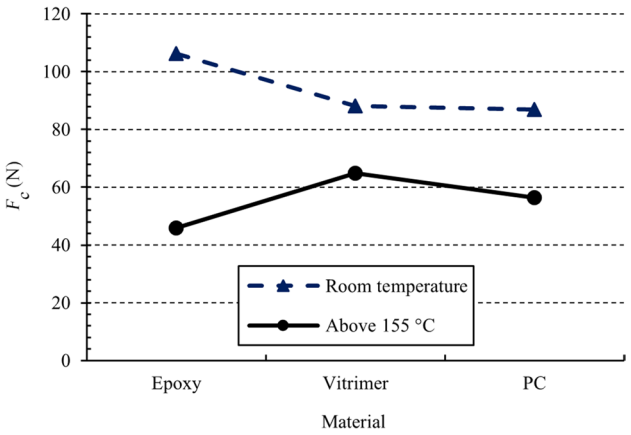

Fig. 6 Interaction plot for main cutting force (F_c) in orthogonal machining of vitrimer, epoxy and PC polymers at room temperature and above the nominal target temperature of 155 °C

analysis of variance (ANOVA) table in Table 4 shows that the influence of the temperature on the F_c is significant; however, neither the material nor the interaction of material vs temperature has a significant effect on the main cutting force at the significance level of 0.05.

3.2 Analysis of surface characteristics

Figure 4 shows the mean of measured surface roughness (Ra) and maximum height of profile (Rt) values of the machined surfaces (machined at room temperature and above 155 °C) of vitrimer, epoxy and PC polymers; the error bar of a total of one sigma (equals the standard deviation) is also shown. In the case of room temperature machining, epoxy samples have the largest average Ra and Rt values, followed by the

Table 4 ANOVA table for main cutting force (F_c), where bold entries denote *P*-values lower than 0.05, indicating that the factor has a significant effect

Source	DF	Adj SS	Adj MS	*F*-value	*P*-value
Model	5	12879.200	2575.800	1.380	0.266
Linear	3	10945.400	3648.500	1.960	0.147
M	2	141.900	71.000	0.040	0.963
T	1	10803.500	10803.500	5.8000	**0.024**
2-way interactions	2	1933.800	966.900	0.520	0.601
M·T	2	1933.800	966.900	0.520	0.601
Error	24	44677.000	1861.500		
Total	29	57556.200			

vitrimer and PC polymers. The epoxy's surface quality indicators are 5–8 times larger than that of the vitrimer's and PC's; however, the difference between vitrimer and PC is much smaller (Ra and Rt of vitrimers are approx. 2 times larger than that of PC). Therefore, the vitrimer's machined surface quality is more similar to the chosen thermoplastic material's than the thermoset epoxy's during machining below the materials' T_g temperature, which is the opposite of the expected result based on the priory mechanical and material properties. This phenomenon should be examined also in detail in future research. The same tendency can be observed at elevated temperature machining: epoxy has the largest surface quality indicator values, followed by vitrimer and PC. But, the difference between epoxy and vitrimer is smaller than between vitrimer and PC this time, which suggests that in the case of machining above the materials' T_g temperature, the vitrimer's machined surface quality is more similar to the chosen thermoset epoxy's than the thermoplastic PC's, which is the opposite of the expected result based on the priory mechanical and material properties. This phenomenon should be examined in detail in future research. From the data, it can be observed that increased temperature has the same effect on decreasing the surface quality (i.e., increasing the Ra and Rt) in the case of vitrimer and epoxy samples; however, an opposite tendency is associated with PC samples. Also, temperature elevation influences the vitrimer and epoxy samples by increasing the standard deviation of the surface roughness values, which means that a more chaotic process occurs during the chip removal above T_g, making the machining outcome more unpredictable. The opposite effect can be seen for PCs in the same machining conditions. These observations suggest that the vitrimers' temperature-dependent behaviour during machining is more similar to the thermoset epoxy than the thermoplastic PC regarding the machined surface's quality.

The connection between the average surface roughness and the maximum height of the profile (i.e., Ra vs Rt) is illustrated in a scatterplot diagram in Fig. 7. All the measured values are presented in the scatterplot (the surface profile of each machined sample was measured three times in three different representative locations), and linear trendlines are also fitted to the different samples' data. The Rt/Ra ratio gives information about the surface damage: the meaning of the high Rt/Ra ratio is the small extent but large size craters on the machined surface (i.e., a small number of large extremes in the surface profile), while the low Rt/Ra ratio suggest that the machined surface is more homogenous with small damages. The Rt/Ra ratios of epoxy machined at both temperature levels and vitrimer machined above 155 °C can be found in the same region in the scatterplot (Group I), the Rt/Ra ratios of PC machined at both temperature levels and vitrimer machined at room temperature can be found in another significantly different region in the scatterplot

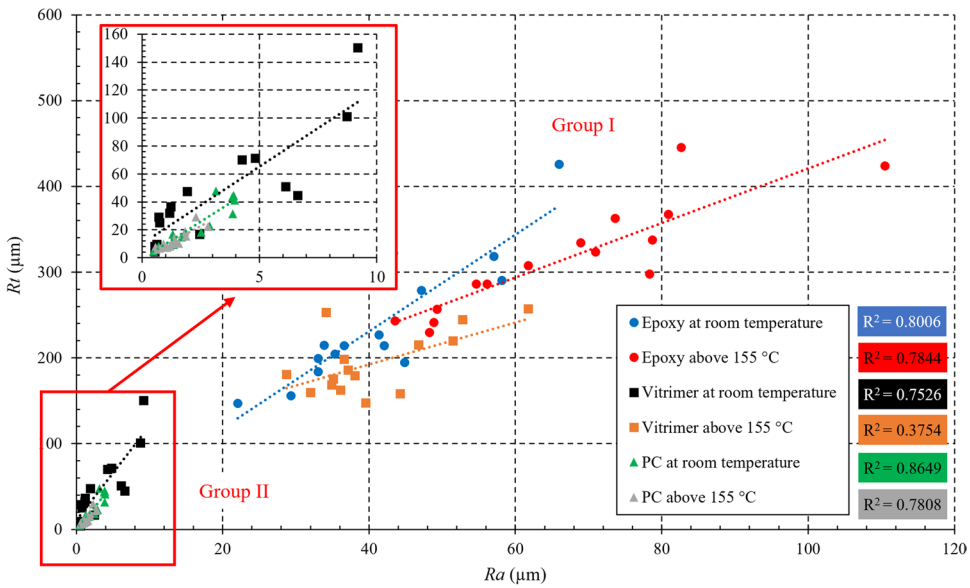

Fig. 7 Scatterplot of average surface roughness (Ra) vs the maximum height of the profile (Rt) of orthogonally machined surfaces of vitrimer, epoxy and PC polymers at room temperature and above 155 °C

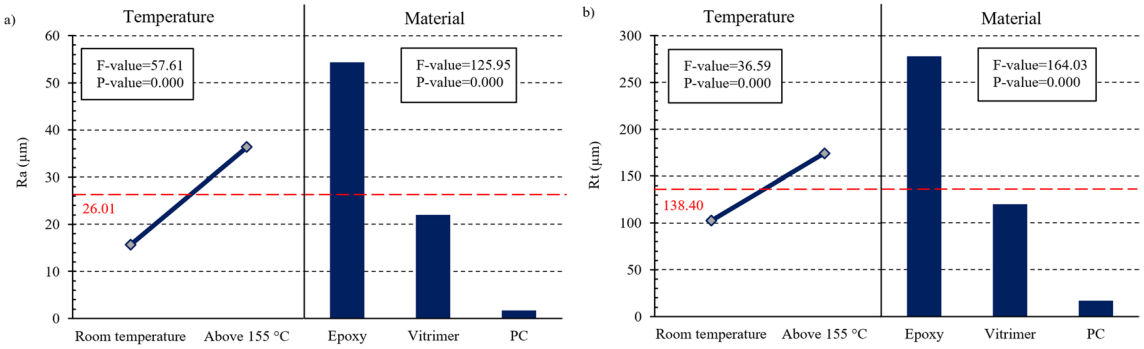

Fig. 8 Main effects plot for **a** average surface roughness (Ra) and **b** maximum height of the profile (Rt) in orthogonal machining of vitrimer, epoxy and PC polymers at room temperature and above the nominal target temperature of 155 °C

(Group II). Moreover, Rt/Ra ratios of elevated temperature machined vitrimer are much closer to the room temperature machined epoxies than the elevated temperature machined epoxy samples in the Group I region. These suggest the similarities between the vitrimer samples machined at different temperature levels and the thermoset epoxy and thermoplastic PC. The range of Ra values of epoxy samples and elevated temperature machined vitrimer samples are much wider compared to the PC samples and room temperature machined vitrimer samples. Also, the same tendency can be observed in the case of the range width of Rt values. These tendencies can be a representation of the machined surface homogeneity: wider ranges suggest a more unpredictable, inhomogeneous surface characteristic. The slope values of the linear fitted trendlines of Group II are higher than in the case of Group I Rt/Ra values of PC samples machined at room temperature have the highest coefficient of determination (R^2), the lowest R^2 belongs to the Rt/Ra values of vitrimer samples machined above 155 °C.

The main effect plots can be seen in Fig. 8. The means in Fig. 8 confirm the previously written observations and statements; the means of the Ra and the Rt of vitrimer, epoxy and PC do differ significantly, also, the larger the cutting temperature, the worse the machined surface quality. The analysis of variances (ANOVA) tables in Tables 5 and 6 shows that the influence of the temperature and the type of material on the Ra and Rt is significant at the significance level of 0.05. The interaction plots of material vs temperature can be seen in Fig. 9. The ANOVA table results (in Tables 5 and 6) and the interaction plots show that the interaction of material vs temperature also has a significant effect on the surface quality (i.e., Ra and Rt values) at the significance level of 0.05. The different materials behave differently with the increase of the temperature, the behaviour of vitrimer and epoxy is more or less similar to each other, but the thermoplastic PC is remarkably different to them.

Table 5 ANOVA table for the average surface roughness (Ra), where bold entries denote *P*-values lower than 0.05, indicating that the factor has a significant effect

Source	DF	Adj SS	Adj MS	*F*-value	*P*-value
Model	5	19201.000	3840.250	68.690	0.000
Linear	3	17303.000	5767.770	103.170	0.000
M	2	14082.000	7041.230	125.950	**0.000**
T	1	3221.000	3220.860	57.610	**0.000**
2-way interactions	2	1898.000	948.980	16.980	0.000
M·T	2	1898.000	948.980	16.980	**0.000**
Error	24	1342.000	55.900		
Total	29	20543.000			

Table 6 ANOVA table for the maximum height of the profile (Rt), where bold entries denote *P*-values lower than 0.05, indicating that the factor has a significant effect

Source	DF	Adj SS	Adj MS	*F*-value	*P*-value
Model	5	414636.000	82927.000	78.760	0.000
Linear	3	383929.000	127976.000	121.550	0.000
M	2	345408.000	172704.000	164.030	**0.000**
T	1	38521.000	38521.000	36.590	**0.000**
2-way interactions	2	30707.000	15354.000	14.580	**0.000**
M·T	2	30707.000	15354.000	14.580	**0.000**
Error	24	25270.000	1053.000		
Total	29	439906.000			

The surface characteristics of the polymer samples were also examined through optical microscopy qualitatively after machining; the representative microscopic images of machined surfaces can be seen in Fig. 10. In the case of epoxy at both temperature levels, a brittle fractured surface can be observed (see in Fig. 10a); furthermore, the extent of craters on the surface increases with temperature increase,

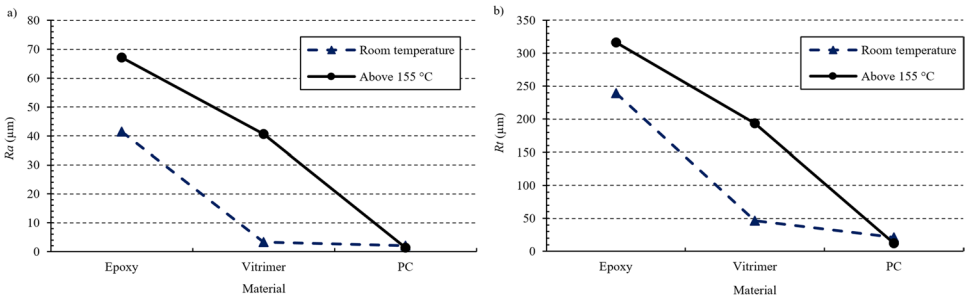

Fig. 9 Interaction plot for **a** average surface roughness (Ra) and **b** maximum height of the profile (Rt) in orthogonal machining of vitrimer, epoxy and PC polymers at room temperature and above 155 °C

which can be a result of the deterioration of mechanical properties above T_g. Regarding the PC's surface characteristics in both temperature levels, a smooth machined surface can be seen (as in Fig. 10c), which can result from plastic deformations during the chip removal process. It also needs to be highlighted that visible grooves parallel to the direction of the tool movement were formed in the case of orthogonal machining above 155 °C; the deterioration of surface quality may be, therefore, a result of decreased mechanical properties above the material's T_g. As for vitrimer (see Fig. 10b), two significantly different surface characteristics can be inspected: (i) at room temperature, a smooth surface without almost any severe surface damage was formed during the orthogonal machining process (similar to the thermoplastic

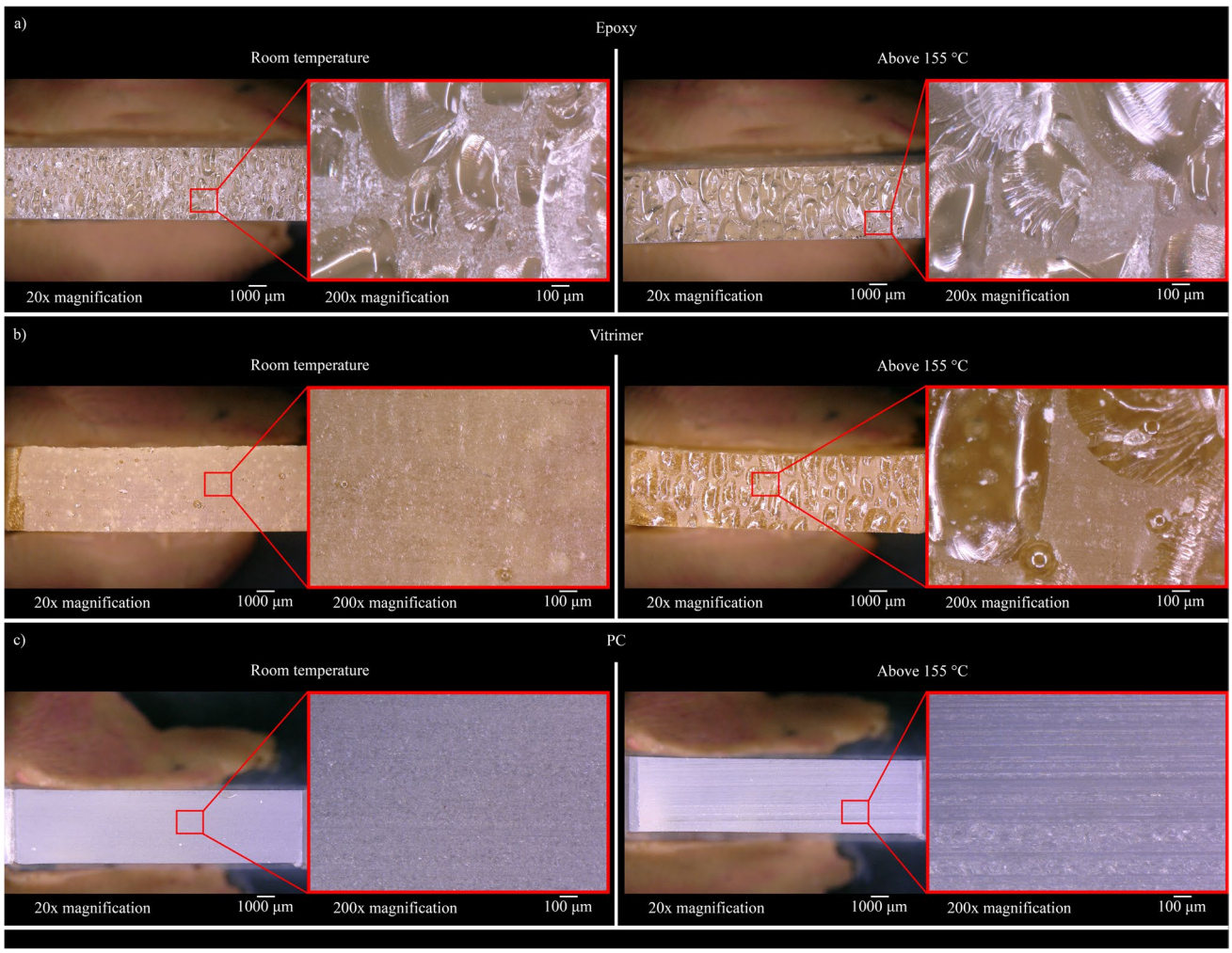

Fig. 10 Representative microscopic images on the machined surfaces of examined **a** epoxy, **b** vitrimer and **c** PC polymers at room temperature and above 155 °C

PC's surface characteristic); however, (ii) above 155 °C, machining a brittle fractured surface was developed (similarly to the thermoset epoxy's surface characteristic). The number and extent of craters on the above T_g machined surface of vitrimer are closer to the case of room temperature machined epoxy; the smooth surface may indicate plastic deformation during material removal. The phenomenon of the embrittlement of the vitrimer as the effect of increasing temperature (inferred from the surface characteristics derived from optical microscopy) needs to be examined in future research.

The achieved significantly better-machined surface quality (regarding Ra and Rt) of polyimine vitrimer samples compared to PER epoxy samples suggests that vitrimers can be a substitute material for commercial epoxies from the point of view of machinability. The machined surface quality is no limit to the widespread use of vitrimers; moreover, better results could be achieved with them than with epoxies. Also, a better surface quality was produced at room temperature during orthogonal machining; therefore, the authors suggest keeping the cutting temperature well below the material's T_g by proper technology planning (e.g., applying coolant, sharp and coated tools, shorter contact time, shorter contact length and optimised cutting parameters). The similarities between the temperature-dependent behaviour of thermoset, thermoplastic and vitrimer materials from the perspective of machined surface characteristics should be further investigated.

3.3 Discussion and outlook

The mechanical and thermal properties of polymer materials are highly affected by the structure of the material. In thermoplastic materials (such as PC), the polymer chains are connected via intermolecular electrostatic forces (e.g., Van der Waals and hydrogen bonding) that are significantly weaker than the primary chemical bonds. Thermosetting polymers (such as PER epoxy) have strong covalent bonds between the polymer chains, which form an irreversible crosslinking network of the molecules in the material. Therefore, thermosetting polymers usually have higher strength and brittle material properties, while thermoplastics can be more deformable and weaker. Polyimine vitrimer polymers, however, have a covalent adaptable network (CAN), which means that dynamic covalent connections are formed between the polymer chains, and the CAN can dynamically rearrange while maintaining the crosslink density when thermally triggered [14]. This results in a special viscoelastic state of the material above the vitrimeric transition temperature [15]. In the case of thermosets and vitrimers, the crosslink density also highly affects the materials' strength [44]. The crosslink density of the polyimine vitrimer used in our experiments might be less than the manufactured PER epoxy's. This theory is supported by the mixing ratios of the different materials: the polyimine vitrimer has an imine–epoxy ratio of 2:1 (in this system, the imine is responsible for the vitrimeric function) and the PER epoxy has an epoxy–hardener ratio of 100:40. The crosslink density can be further analysed by Differential Scanning Calorimetry (DSC). The storage modulus values (E') from DMA tests (see Table 1) clearly show the differences between the materials: the thermoset PER epoxy has the highest E' at room temperature, followed by the polyimine vitrimer with the lower crosslink density, and the thermoplastic PC has the lowest E'. The mechanical properties of polymers are also highly influenced by temperature. The mechanical properties of thermosets, thermoplastics and vitrimers significantly deteriorate as the temperature exceeds the glass transition temperature (T_g) due to the micro-Brownian motion of the macromolecules. This deterioration tendency can also be observed from the results of the DMA tests (see Table 1). The extremely low value of the polyimine vitrimer may indicate that the temperature exceeded the vitrimeric transition temperature (T_v).

The main cutting force (F_c) values of the different materials are in correlation with the mechanical properties of the material and the above-mentioned theoretical statements. As the polyimine vitrimer has less crosslink density at room temperature, the F_c values are closer to the F_c values of the PC than of the epoxy. In the case of elevated temperature machining, the F_c values of each material decreased due to the deterioration of the mechanical properties as expected. The polyimine vitrimer had the highest F_c values at elevated temperatures which may be explained by the higher resistance against the main cutting edge of the viscoelastic material state compared to the rigid but weakened epoxy and PC. As the thermosets have a brittle nature and higher strength due to the strong covalent bonds between the polymer chains, the surface roughness should be worse than in the case of the thermoplastics that have a softer and more ductile nature due to the secondary chemical bonds between the polymer chains [45–47]. As it is harder to separate the molecules during the cutting process, the thermosets should have more brittle fractured surface characteristics [45, 46]; however, the thermoplastics should have smoother surface characteristics due to weak intermolecular forces [46, 47]. The results of this study's surface roughness and characteristics resemble the theoretically expected and previous research results. As there is no published information on the vitrimers' behaviour during machining, the findings of the surface roughness and characteristics analysis are unique: at room temperature, the used polyimine vitrimer has a smooth surface finish similar to the PC, but above T_g, the surface is more similar to the epoxy's. The similarity to PC may be explained by the lower crosslink density; however, the material still has a crosslinking network above T_g; therefore,

a brittle fractured machined surface appears similar to the epoxy. The machining-induced surface characteristics-related priori information on the crosslink density dependency and the temperature dependency (i.e., exceeding T_g) is also consistent with the results [46].

In this research, two polymer materials (PER epoxy and PC) similar in thermomechanical properties to the examined polyimine vitrimer were applied as comparative references. However, a wide range of thermosetting polymer materials are used in today's industrial applications with different mechanical and thermal properties; also, vitrimer materials can be synthesised in many different ways, which also affects the properties of the material. As vitrimers are potential substitution materials for conventional thermosets (e.g., epoxies), more comparative experiments should be carried out on different materials to map the similarities and differences in the case of machining. Furthermore, the main area of use of conventional thermoset and polyimine vitrimer materials are fibre-reinforced composites, not used by themselves in solid form. Therefore, orthogonal machining experiments should be performed on vitrimer matrix FRP composites to investigate and model the machinability of industry potential materials and analyse the effect of fibre–vitrimer adhesion on machinability.

The different recycling methods (i.e., mechanical, chemical and thermal) can affect the material properties of the recovered materials. The high-temperature treatment during pyrolysis and the mechanical impacts during the recycling procedure can affect the tensile properties and fatigue resistance of the reinforcement; furthermore, the chemicals applied during solvolysis can affect the adhesion between the matrix and reinforcement. While mechanical properties and adhesion can play a significant role in the outcome of the machining process, the authors plan to examine and compare the machined features' quality and the affected optimisation parameters of the machining process in the case of composites prepared from virgin and recycled materials.

Vitrimer materials have three significant and distinguishable temperature zones: (i) operating temperature zone (below glass transition temperature (T_g) and vitrimeric transition temperature (T_v)), (ii) mechanical characteristics deterioration temperature zone (between T_g and T_v) and (iii) viscoelastic flow temperature zone (above T_v). In these temperature zones, the vitrimer may behave significantly differently during machining; therefore, further research should aim to discover the processes taking place during machining. For these experiments, the vitrimeric transition temperature should be determined appropriately. In our orthogonal machining experiments, the cutting tool was heated above the target elevated temperature; however, heat transfer properties and heat conductivity of the different materials (experimental samples and cutting tool) were not investigated and taken into consideration. Also, the contact time of the cutting tool and experimental samples was short (approx. 0.05 s); nevertheless, experimental results clearly show the different outcomes of the separate temperature levels. Even so, in our further experiments, direct heating of the samples will be applied to validate the recent data.

In the recent machining experiments, the applied cutting speed was the milling machine's rapid speed of 20 m/min, which is a common limitation of orthogonal machining experiments [48, 49]; however, other commonly applied machining operations (e.g., milling and drilling) have a several times higher cutting speed. Recent results may be extended to higher cutting speed processes, although validating experiments must be carried out in further research. The results and experience of this orthogonal machining experiment can be directly implemented in other machining operations, where no rotating cutting tool is applied, the direction vector of the cutting speed is constant, and a homogenous chip cross-section is maintained during the machining process, such as turning, planing, shaping, and broaching; however, the implementation to other machining operations with more complex kinematics (e.g., milling and drilling) is highly limited. Therefore, in future applied machining research, these more complex, typically used machining processes in the industry should be examined to help spread vitrimer matrix FRP materials in industrial production. The implementation of the experimental results is also limited due to the geometry of the cutting tool insert and the number of cutting edges. In the case of different cutting tool geometries, the peel-up and ploughing effect may appear in varying degrees; also, the increase in the number of cutting edges changes the chip-removal kinematics significantly. These effects significantly influence the cutting forces and the machined surface quality; therefore, further experimental research and modelling should be conducted. Additionally, the short length and the simple tool path of the orthogonal cut are drawbacks of recent experiments, while other extensive surface characteristics, such as waviness and flatness, cannot be determined. In the case of multiple paths operations, the errors of previous paths may significantly influence the result of the following tool paths. Recent results must be interpreted in dry machining conditions, although coolant fluid highly affects the temperature and tribological conditions. However, the applicability of coolant fluids must be investigated in future research.

4 Conclusions

In the present study, a comparative analysis of the machinability of polyimine vitrimer, thermoset PER epoxy and thermoplastic polycarbonate was carried out by orthogonal

cutting experiments to have preliminary information on the behaviour of vitrimer polymers during machining. The machinability was examined by analysing cutting forces, surface roughness and surface characteristics. According to the present study, the following conclusions can be drawn:

- Experimental results show that polyimine vitrimer produced smaller cutting forces (i.e., main cutting force component (F_c) and passive force component (F_p)) than the PER epoxy. Thus, vitrimer materials may be more favourable from the perspective of machining due to the smaller tool wear and permanent mechanical damage caused by the F_c. Cutting force results also show that the force component values and their deviation increase with the increase in temperature; therefore, cutting temperature control is recommended.
- Surface roughness indicators (i.e., average surface roughness (Ra) and maximum height of profile (Rt)) show the machined surface of polyimine vitrimer was better quality than PER epoxy's machined surface; therefore, vitrimer materials may be a good substitute of epoxies from the perspective of machined surface quality. However, optical microscopy images showed that at room temperature machining polyimine vitrimer's machined surface was similar to the thermoplastic polycarbonate's machined surface, but above the glass transition temperature (T_g), the machined surface of vitrimer was similar to the thermoset PER epoxy's machined surface.
- ANOVA results show that temperature had a significant effect on the main cutting force component and the surface quality; also, the material factor and the interaction of the material vs temperature on the surface quality was significant at the significance level of 0.05.
- The preliminary experimental results of the comparative analysis of the machinability of vitrimers are limited because of the chosen materials and the orthogonal machining; more empirical work is therefore needed in order to thoroughly investigate and compare the machinability of different types of vitrimers and epoxies also to get information on the commonly applied machining operations in the industry (e.g., milling and drilling) and to investigate the more complex processes, which happens during the machining of vitrimer matrix fibre-reinforced polymer composites.

Acknowledgements The authors acknowledge the technical support of Tamás Lukács, Bertalan Papp, Márton Csillik and Boglárka Devecser in preparation works.

Author contribution Dániel István Poór: Conceptualization, methodology, software, formal analysis, investigation, data curation, writing—original draft and visualization. Marina Tobey: investigation and writing—review and editing. Philip Taynton: resources and writing—review and editing. Ákos Pomázi: investigation, resources and writing—review and editing. Andrea Toldy: validation, resources, and writing—original draft and funding acquisition. Norbert Geier: conceptualization, methodology, validation, formal analysis, resources, writing—original draft, supervision and funding acquisition.

Funding Open access funding provided by Budapest University of Technology and Economics. This research was implemented thanks to the support of the 2021-1.2.4-TÉT-2021-00050, which encourages scientific and technological cooperation between USA and Hungary. Supported by the ÚNKP-22-3-I-BME-92 and ÚNKP-23-5-3502 New National Excellence Program of the Ministry for Culture and Innovation from the source of the National Research, Development and Innovation Fund. This research was partly supported by the János Bolyai Research Scholarship of the Hungarian Academy of Sciences No. BO/00508/22/6. This research was funded by the National Research, Development and Innovation Office (2018-1.3.1-VKE-2018-00011 and NKFIH K142517).

Declarations

Competing interests The authors declare the following financial interests/personal relationships which may be considered as potential competing interests: Philip Taynton reports a relationship with Mallinda Inc. that includes equity or stocks. Marina Tobey reports a relationship with Mallinda Inc. that includes employment. Philip Taynton has patent Anhydrous routes to highly processable covalent network polymers and blends with royalties paid to Mallinda Inc.

References

1. Lukács T, Pereszlai C, Geier N (2023) Delamination measurement in glass fibre reinforced polymer (GFRP) composite based on image differencing. Compos B Eng 248:110381. https://doi.org/10.1016/j.compositesb.2022.110381
2. Magyar G, Geier N (2023) Analysis and modelling of thrust force in drilling of basalt and carbon fibre-reinforced polymer (BFRP and CFRP) composites. J Braz Soc Mech Sci Eng 45:323. https://doi.org/10.1007/s40430-023-04241-7
3. Forintos N, Czigany T (2019) Multifunctional application of carbon fiber reinforced polymer composites: electrical properties of the reinforcing carbon fibers – a short review. Compos B Eng 162:331–343. https://doi.org/10.1016/j.compositesb.2018.10.098
4. Szebényi G (2022) High-performance composites and medical applications of polymers – the sunny side of the polymer industry. Express Polym Lett 16:1113–1113. https://doi.org/10.3144/expresspolymlett.2022.81
5. Tamás-Bényei P, Sántha P (2023) Potential applications of basalt fibre composites in thermal shielding. J Therm Anal Calorim 148:271–279. https://doi.org/10.1007/s10973-022-11799-2

6. Geier N, Poór DI, Pereszlai C, Tamás-Bényei P, Xu J (2022) A drilling case study in polymer composites reinforced by virgin and recycled carbon fibres (CFRP and rCFRP) to analyse thrust force and torque. Int J Adv Manuf Technol 120:2603–2615. https://doi.org/10.1007/s00170-022-08947-1
7. Rani M, Choudhary P, Krishnan V, Zafar S (2021) A review on recycling and reuse methods for carbon fiber/glass fiber composites waste from wind turbine blades. Compos B Eng 215:108768. https://doi.org/10.1016/j.compositesb.2021.108768
8. Toldy A (2021) Recyclable-by-design thermoset polymers and composites. Express Polym Lett 15:1113–1113. https://doi.org/10.3144/expresspolymlett.2021.89
9. Xu Z, Liang Y, Ma X, Chen S, Yu C, Wang Y, Zhang D, Miao M (2020) Recyclable thermoset hyperbranched polymers containing reversible hexahydro-s-triazine. Nat Sustain 3:29–34. https://doi.org/10.1038/s41893-019-0444-6
10. The European Parliament and The Council of the European Union (2008) Directive 2008/98/EC. Directive 2008/98/EC of the European Parliament and of the Council of 19 November 2008 on waste and repealing certain Directives (Text with EEA relevance). http://data.europa.eu/eli/dir/2008/98/oj/eng. Accessed 31 Aug 2023
11. Toldy A (2023) Challenges and opportunities of polymer recycling in the changing landscape of European legislation. Express Polym Lett 17:1081–1081. https://doi.org/10.3144/expresspolymlett.2023.81
12. Balaji AB, Rudd C, Liu X (2020) Recycled carbon fibers (rCF) in automobiles: towards circular economy. Mater Circ Econ 2:4. https://doi.org/10.1007/s42824-020-00004-0
13. Geier N, Poór DI, Pereszlai C, Tamás-Bényei P (2022) Drilling of recycled carbon fibre–reinforced polymer (rCFRP) composites: analysis of burrs and microstructure. Int J Adv Manuf Technol 120:1677–1693. https://doi.org/10.1007/s00170-022-08847-4
14. Montarnal D, Capelot M, Tournilhac F, Leibler L (2011) Silica-like malleable materials from permanent organic networks. Science 334:965–968. https://doi.org/10.1126/science.1212648
15. Denissen W, Winne JM, Du Prez FE (2016) Vitrimers: permanent organic networks with glass-like fluidity. Chem Sci 7:30–38. https://doi.org/10.1039/C5SC02223A
16. Taynton P, Yu K, Shoemaker RK, Jin Y, Qi HJ, Zhang W (2014) Heat- or water-driven malleability in a highly recyclable covalent network polymer. Adv Mater 26:3938–3942. https://doi.org/10.1002/adma.201400317
17. Taynton P, Ni H, Zhu C, Yu K, Loob S, Jin Y, Qi HJ, Zhang W (2016) Repairable woven carbon fiber composites with full recyclability enabled by malleable polyimine networks. Adv Mater 28:2904–2909. https://doi.org/10.1002/adma.201505245
18. Taynton P, Luo Y, Rubin H, Kissounko D, Loob S, Sadowski S (2020) Anhydrous routes to highly processable covalent network polymers and blends. US20200247937A1. https://patents.google.com/patent/US20200247937A1/en. Accessed 27 Dec 2023
19. Technical Committee ISO/TC 61, Plastics, Subcommittee SC 5, Physical-chemical properties, European Committee for Standardization (CEN) Technical Committee CEN/TC 249, Plastics (2020) ISO 11357-2:2020, Plastics — Differential scanning calorimetry (DSC) — Part 2: Determination of glass transition temperature and step height. https://www.iso.org/standard/77310.html. Accessed 27 Dec 2023
20. Hagen R, Salmén L, Lavebratt H, Stenberg B (1994) Comparison of dynamic mechanical measurements and Tg determinations with two different instruments. Polym Testing 13:113–128. https://doi.org/10.1016/0142-9418(94)90020-5
21. Yang Y, Zhang S, Zhang X, Gao L, Wei Y, Ji Y (2019) Detecting topology freezing transition temperature of vitrimers by AIE luminogens. Nat Commun 10:3165. https://doi.org/10.1038/s41467-019-11144-6
22. Schenk V, Labastie K, Destarac M, Olivier P, Guerre M (2022) Vitrimer composites: current status and future challenges. Mater Adv 3:8012–8029. https://doi.org/10.1039/D2MA00654E
23. Van Zee NJ, Nicolaÿ R (2020) Vitrimers: permanently crosslinked polymers with dynamic network topology. Prog Polym Sci 104:101233. https://doi.org/10.1016/j.progpolymsci.2020.101233
24. Natarajan E, Kaviarasan V, Ang KM, Lim WH, Elango S, Tiang SS (2022) Production wastage avoidance using modified multi-objective teaching learning based optimization embedded with refined learning scheme. IEEE Access 10:19186–19214. https://doi.org/10.1109/ACCESS.2022.3151088
25. Popan IA, Balc N, Popan AI (2022) Avoiding carbon fibre reinforced polymer delamination during abrasive water jet piercing: a new piercing method. Int J Adv Manuf Technol 119:1139–1152. https://doi.org/10.1007/s00170-021-08294-7
26. Wang F, Yin J, Ma J, Jia Z, Yang F, Niu B (2017) Effects of cutting edge radius and fiber cutting angle on the cutting-induced surface damage in machining of unidirectional CFRP composite laminates. Int J Adv Manuf Technol 91:3107–3120. https://doi.org/10.1007/s00170-017-0023-9
27. Qin X, Bao Z, Wu W, Li H, Li S, Zhao Q (2022) Surface quality evaluation for CFRP milling and its impact on the mechanical properties. Int J Adv Manuf Technol 122:1083–1097. https://doi.org/10.1007/s00170-022-09942-2
28. Zhang D, Wang H, Burks AR, Cong W (2020) Delamination in rotary ultrasonic machining of CFRP composites: finite element analysis and experimental implementation. Int J Adv Manuf Technol 107:3847–3858. https://doi.org/10.1007/s00170-020-05310-0
29. Fu G, Sun F, Huo D, Shyha I, Sun F, Fang C (2021) FE-simulation of machining processes of epoxy with Mulliken Boyce model. J Manuf Process 71:134–146. https://doi.org/10.1016/j.jmapro.2021.09.026
30. Wang H, Chang L, Mai Y-W, Ye L, Williams JG (2018) An experimental study of orthogonal cutting mechanisms for epoxies with two different crosslink densities. Int J Mach Tools Manuf 124:117–125. https://doi.org/10.1016/j.ijmachtools.2017.10.003
31. Rong Y, Wang L, Zhang T, Li M, Huang Y, Zhang G, Wu C (2021) Precision cutting of epoxy resin board (ERB) by ultraviolet (UV) nanosecond laser ablation with consideration of hazardous gas protection. Optik 241:167154. https://doi.org/10.1016/j.ijleo.2021.167154
32. Alauddin M, Choudhury IA, El Baradie MA, Hashmi MSJ (1995) plastics and their machining: a review. J Mater Process Technol 54:40–46. https://doi.org/10.1016/0924-0136(95)01917-0
33. Muqeet A, Israr A, Zafar MH, Mansoor M, Akhtar N (2023) A novel optimization algorithm based PID controller design for real-time optimization of cutting depth and surface roughness in finish hard turning processes. Results Eng 18:101142. https://doi.org/10.1016/j.rineng.2023.101142
34. Singh R (2022) On electro-chemical machining of thermosetting polymer matrix. In: Hashmi MSJ (ed) Encyclopedia of Materials: Plastics and Polymers. Elsevier, Oxford, pp 436–443. https://doi.org/10.1016/B978-0-12-820352-1.00147-4
35. Wang H, Chang L, Ye L, Williams JG (2015) On the toughness measurement for ductile polymers by orthogonal cutting. Eng Fract Mech 149:276–286. https://doi.org/10.1016/j.engfracmech.2015.06.067
36. Hanson C, Hiwase P, Chen X, Jahan MP, Ma J, Arbuckle G (2019) Experimental investigation and numerical simulation of burr formation in micro-milling of polycarbonates. Procedia Manuf 34:293–304. https://doi.org/10.1016/j.promfg.2019.06.153
37. Sidiq P, Abdalrahman RM, Rostam S (2020) Optimizing the simultaneous cutting-edge angles, included angle and nose radius

for low cutting force in turning polyamide PA66. Results Mater 7:100100. https://doi.org/10.1016/j.rinma.2020.100100
38. Geier N, Davim JP, Szalay T (2019) Advanced cutting tools and technologies for drilling carbon fibre reinforced polymer (CFRP) composites: a review. Compos A Appl Sci Manuf 125:105552. https://doi.org/10.1016/j.compositesa.2019.105552
39. Geier N, Xu J, Poór DI, Dege JH, Davim JP (2023) A review on advanced cutting tools and technologies for edge trimming of carbon fibre reinforced polymer (CFRP) composites. Compos B Eng 266:111037. https://doi.org/10.1016/j.compositesb.2023.111037
40. Ashworth S, Fairclough JPA, Meredith J, Takikawa Y, Kerrigan K (2022) Effects of tool coating and tool wear on the surface quality and flexural strength of slotted CFRP. Wear 498–499:204340. https://doi.org/10.1016/j.wear.2022.204340
41. Xu J, Lin T, Davim JP, Chen M, El Mansori M (2021) Wear behavior of special tools in the drilling of CFRP composite laminates. Wear 476:203738. https://doi.org/10.1016/j.wear.2021.203738
42. Sauer K, Witt M, Putz M (2019) Influence of cutting edge radius on process forces in orthogonal machining of carbon fibre reinforced plastics (CFRP). Procedia CIRP 85:218–223. https://doi.org/10.1016/j.procir.2019.09.042
43. Sauer K, Nowak A, Regel J, Wertheim R, Dix M (2021) Geometric empirical modelling of forces influenced by the cutting edge microgeometry in orthogonal cutting of unidirectional CFRP. Procedia CIRP 102:25–30. https://doi.org/10.1016/j.procir.2021.09.005
44. Huang J, Fu P, Li W, Xiao L, Chen J, Nie X (2022) Influence of crosslinking density on the mechanical and thermal properties of plant oil-based epoxy resin. RSC Adv 12:23048–23056. https://doi.org/10.1039/D2RA04206A
45. Fu G, Huo D, Shyha I, Sun F, Gao Q (2022) Machinability investigation of polymer/GNP nanocomposites in micro-milling. Int J Adv Manuf Technol 119:2341–2353. https://doi.org/10.1007/s00170-021-08471-8
46. Carr JW, Feger C (1993) Ultraprecision machining of polymers. Precis Eng 15:221–237. https://doi.org/10.1016/0141-6359(93)90105-J
47. Uchiyama R, Inoue Y, Uchiyama F, Matsumura T (2021) Optimization in milling of polymer materials for high quality surfaces. Int J Autom Technol 15:512–520. https://doi.org/10.20965/ijat.2021.p0512
48. Yan X, Reiner J, Bacca M, Altintas Y, Vaziri R (2019) A study of energy dissipating mechanisms in orthogonal cutting of UD-CFRP composites. Compos Struct 220:460–472. https://doi.org/10.1016/j.compstruct.2019.03.090
49. Hou G, Luo B, Zhang K, Luo Y, Cheng H, Cao S, Li Y (2021) Investigation of high temperature effect on CFRP cutting mechanism based on a temperature controlled orthogonal cutting experiment. Compos Struct 268:113967. https://doi.org/10.1016/j.compstruct.2021.113967